2025-01-8020 Published 01 Apr 2025

Machine Learning-Based Lane Detection and Lateral Offset Estimation Model for Vehicle Following Applications

Nirmal Raja Karuppiah Loganathan, Aman Poovalappil, Jeffrey Naber, Darrell Robinette, and Mojtaba Bahramgiri Michigan Technological University

Citation: Karuppiah Loganathan, N. R., Poovalappil, A., Naber, J., Robinette, D. et al., "Machine Learning-Based Lane Detection and Lateral Offset Estimation Model for Vehicle Following Applications," SAE Technical Paper 2025-01-8020, 2025, doi:10.4271/2025-01-8020.

Received: 29 Oct 2024 Revised: 19 Dec 2024 Accepted: 21 Jan 2025

Abstract

Precisely understanding the driving environment and determining the vehicle's accurate position is crucial for a safe automated maneuver. vehicle following systems that offer higher energy efficiency by precisely following a lead vehicle, the relative position of the ego vehicle to lane center is a key measure to a safe automated speed and steering control. This article presents a novel Enhanced Lane Detection technique with centimeter-level accuracy in estimating the vehicle offset from the lane center using the front-facing camera. Leveraging state-of-the-art computer vision models, the Enhanced Lane Detection technique utilizes YOLOv8 image segmentation, trained on a diverse world driving scenarios dataset, to detect the driving lane. To measure the vehicle lateral offset, our model introduces a novel calibration method using nine reference markers aligned with the vehicle perspective and converts the lane offset from image coordinates to world measurements. This design minimizes the sensitivity of offset estimation to lane detection accuracy and vehicle orientation. Compared to the existing deep learning-based depth perception models and stereo vision systems, our calibration method significantly improves postprocessing time and minimizes the impacts of the processing delay on the vehicle following system energy efficiency. To assess the accuracy and processing time, we implemented the model on an instrumented L4-capable vehicle and conducted automated vehicle following tests in a controlled environment. In our tests, the model achieved a high level of accuracy, with a biased error of only 0.214 m and a random walk error standard deviation of 0.135 m, demonstrating its reliability across various environmental conditions and ensuring precise lane tracking. Results demonstrate reliable performance across various environmental conditions and sensor noise levels, ensuring precise lane tracking and enhanced automated maneuvering.

Introduction

The development of autonomous driving technologies has several challenges, with one of the most critical being the accurate detection of road lanes and estimation of vehicle position with respect to the lane center. Precise lane detection and lateral offset estimation are essential for the safe and efficient operation of Autonomous Vehicles (AVs), especially in vehicle-following systems. AVs can keep a stable position inside their driving lane and accurately track and follow a lead vehicle using these systems. This is fundamental to both energy efficiency and safety as a vehicle can self-correct steering and speed with small adjustments to ensure smooth dynamic maneuvers.

The precise vehicle lateral offset to centerline is a key measure that allows lane level position control and enables advanced vehicle following systems with energy efficiency enhancement purposes [1]. To have an accurate and reliable offset to centerline estimation, we can use various advanced computer vision techniques and lane detection models, with a promising performance; however, depth information, which is required for translating the offset from two-dimensional image coordinate to three-dimensional world coordinate, is missing in a traditional monocular computer vision system. There are various approaches to predict the distance of camera sensor to a detected object within the image frame, including deep learning-based depth perception models [2], stereo vision-based computer vision models, and camera fusion with sensors with other modalities, such as Lidar and radar. However, in offset to centerline estimation for a vehicle, the fixed height of the camera to the ground, in addition to detected lane in image frame can potentially solve the issue with this specific 2D to 3D translation.

In this article we proposed a model, that first utilizes a customized YOLOv8 model to perform lane detection and segmentation. This model is trained on a diverse dataset collected for this study, accurately identifies lane boundaries across various driving conditions, ensuring robust detection. Next, the proposed model applies a

novel nine-point calibration method to compensate for lack of depth information in offset to centerline estimation. Here, we present a methodology that performs precise calculations converting the detected lane offset from image coordinates back to three-dimensional world coordinate with centimeter-level accuracy in estimating lateral offset. The offset is then fed back to the main control system of AVs to adjust steering and speed for the AV to smoothly position itself in the lane for vehicle following application.

The calibration method introduced in this work offers high accuracy in offset to centerline measurement, with considerably low processing delay, which essentially minimizes the impact of lane detection process delay on steering controlling system performance. To integrate the model into an instrumented vehicle, we use Nvidia AGX Orin GPU for accelerated post-processing. This allows the AV to react quickly to changes in the environment and to maintain high-precision lane tracking regardless of varying conditions of illumination, weather, and road quality. To prove the effectiveness of our approach, we integrated our framework on a Level 4 (L4) capable autonomous vehicle and performed numerous tests in a controlled environment. The system is tested under different scenarios with various weather and road conditions and with sensor noise. Our results show that the Enhanced Lane Detection provides consistent lane tracking with centimeter-level accuracy.

The Literature review section reviews existing works that offer offset to centerline estimation. The Methodology section illustrates the design of the model, the calibration, and the lateral offset estimation methodology, and explains the integration of Nvidia GPU to enhance model performance. Also, it covers the testing procedure along with the corresponding reliability of the system.

Literature Review

Lane detection is an important, but critical, aspect of advanced driver assistance systems (ADAS) and autonomous vehicles. Different techniques for tackling challenges like varying weather, lighting conditions, and road complexities have been explored by the researchers. In [3], a fuzzy C-means algorithm was applied to enhance the robustness of lane boundary detection under varying lighting conditions. This method effectively combines spatial information with edge detection, but it is limited in terms of real-time application for high computational overhead. Similarly, In [4], the proposed real-time lane departure warning system utilizes spatiotemporal mechanisms to ensure stable lane detection during both day and night. In this system, high detection accuracy with over 98% lane detection rate under highway conditions was attained. Another method introduced in [5] focuses on using gradient-pair constraints and the Hough Transform to detect lane boundaries. This improves lane detection robustness under complex road environments and decreases the effects of shadows and occlusions. In [6], the developed threshold segmentation-based algorithm performs well in identifying lane lines even in the presence of shadows, though manual parameter adjustments are needed for optimal performance. A novel piecewise linear stretching function (PLSF) was employed in [7] to improve contrast and computational efficiency. The Euclidean distance transform is used in this function to detect lane departures with fewer false alarms. In [8], the proposed piecewise fitting method combines object segmentation with thresholding to detect lane markers accurately in low-light conditions.

Adaptive techniques were explored in [9], which utilized vanishing points to dynamically adjust the region of interest (ROI) for lane detection. This method can adapt to the changing of conditions in roads, which can help increase the accuracy of the detection and increase the efficiency of detection. In [10], the authors further enhanced lane-mark extraction using local edge orientation and Kalman filters to maintain performance under adverse weather conditions.

In [11], the authors demonstrated a video-based lane departure warning system utilizing Hough Transform, emphasizing cost-effective implementation for real-time applications. Meanwhile, In [12], a two-stage feature extraction method with curve fitting was performed to improve lane detection under noisy environments. Both lighting inconsistencies and background clutter are addressed by their model to be robust to lane tracking. In [13], the proposed VioLET system integrates steerable filters to improve the detection of both solid and segmented lane markings. In addition, their work is robust to lighting changes and shadow effects, allowing for very high detection accuracy even in conditions of diverse environments. In [14] the developed lane detection approach using a Catmull-Rom spline model offers a more flexible representation of lanes compared to parabolic models enhancing performance on both marked and unmarked roads. In [15], the authors tackled the challenge of detecting multiple lanes using panoramic cameras, proposing an equidistant curves model. In this model, lanes can have complex curvature, and hence it can be used in urban environments. In [16], the authors focused on nighttime lane detection, combining Canny edge detection with Hough Transform to address uneven illumination and enhance the visibility of lane markings in low-light conditions. Deep learning models have been used recently for lane detection. In [17], the introduced RS-Lane method based on ResNeSt and self-attention distillation shows performance improvements under challenging traffic conditions including shadow occlusions and dazzle light. Similarly, In [18], the LDNet lane marking detection network uses dynamic vision sensors (DVS) to overcome the problems of motion blur and illumination variations and lend itself well to real-time lane detection tasks.

These studies show the development of lane detection technology evolution focusing on robust, real-time performance and adaptability. Our work approach is to utilize the same YOLO8 model for lane segmentation as the method currently in development whereas the novelty

of our approach is in our nine-point calibration. This technique improves precision due to image coordinates' conversion into world units, yielding centimeter-level accuracy, necessary for vehicle following systems. In contrast to previous methods, our calibration strategy has faster processing times and better energy efficiency, and that is unique among existing autonomous vehicle technologies.

Methodology

Here, we present a methodology that employs an accurate and efficient system for lane detection and lateral offset estimation in autonomous vehicle applications. A combination of machine learning, computer vision, and calibration techniques is used to achieve this in real-time and produce robust performance across constantly changing world conditions. As shown in figure 1 this system consists of a Zed 2i camera, Computer Vision Core running on Nvidia Jetson AGX Orin, and an Autonomy Core are connected using a User Datagram Protocol (UDP) interface to ensure real-time communication for vehicle control.

Image Acquisition using Zed 2i Camera – Zed 2i is strategically mounted above the driver's head to get the best front-facing view of the road. In this positioning, we are guaranteed unobstructed visibility of lane boundaries for accurate detection. For the purpose of this model, we only use the right frame. To reduce the computational overhead, each frame is resized to 360x720 pixels while compromising detection quality. The resized frames are then transmitted to the Computer Vision Core for analysis. Computer Vision Core – The Computer Vision Core, powered by Nvidia AGX, is responsible for two significant sub-processes: YOLOv8 Segmentation and Vehicle Offset Estimation.

YOLOv8 Segmentation – The input frame is processed through a custom YOLOv8 model trained using a trained on a diverse dataset collected for this study. This segmentation model predicts the safe driving area within the lane boundaries, and it finds the bounds within which the vehicle has to operate. The subsequent offset estimation is based on this lane detection and the offset accurately tracks the lane center.

Offset Estimation – After the lane boundaries are found the system calculates the lateral offset of the vehicle from the center of the lane. A nine-point calibration method is used to compute this offset and achieve centimeter-level accuracy. Nine reference points align with the vehicle's perspective in the calibration method, converting image coordinates to real-world measurements. The advantage of this approach is that it is robust to mild inaccuracies in detection and vehicle orientation and produces meaningful offset values for lane keeping.

Transmission via UDP Interface – We developed a User Datagram Protocol (UDP) interface to communicate the estimated offset value Computer Vision Core to the Autonomy Core. UDP interface is used for low latency communication which is needed for real-time processing and decision making in dynamic driving scenarios.

Autonomy Core for Speed and Steering Control – Upon receiving the offset values, the Autonomy Core runs adjustments in steering and speed to bring the vehicle up to the center of the lane. These give smooth dynamic maneuvers with less frequent corrections. Stable vehicle-following behavior is ensured and energy efficiency and driving safety are improved by this real-time control. This methodology ensures precise lane detection and offset calculation while maintaining smooth vehicle control, contributing to the safety and efficiency of autonomous driving systems.

Lane Segmentation Model

To train the YOLOv8 model, we collected a dataset using the Zed 2i camera under diverse challenging driving scenarios to ensure the model will be robust in real-world situations. The data was collected across different weather and lighting environments such as normal, underexposed, snow, rain, fog, daytime, and nighttime.

Figure 2 shows sample images from the dataset, demonstrating the variety of conditions the model was trained. The dataset consists of 3,026 images, divided into training, validation, and test sets with an 11:2:1 ratio, comprising 2,400 images (79%) for training, 426 images (14%) for validation, and 200 images (7%) for testing. This split ensures effective training while maintaining enough data for evaluation. We apply pre-processing techniques like auto-orienting the images to achieve a consistent alignment for improving the generalization of the model. Furthermore, we augment 100% of the training data to simulate different real-time conditions. This is augmented by hue (±15°), saturation (±25%), brightness (±15%), exposure (±10%), image blur (up to 2.5 pixels), and image noise (up to 0.1% of pixels). These techniques allow the model to change its behavior depending on the different visibility

FIGURE 1 Enhanced Lane Detection model block diagram and output sample.

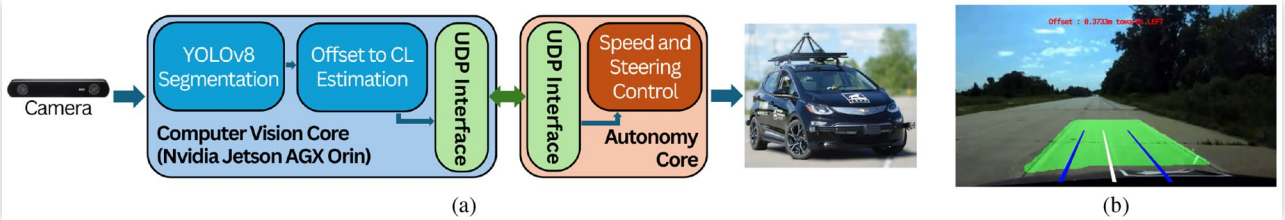

FIGURE 2 Dataset Split and Sample Images Captured in Diverse Driving Conditions

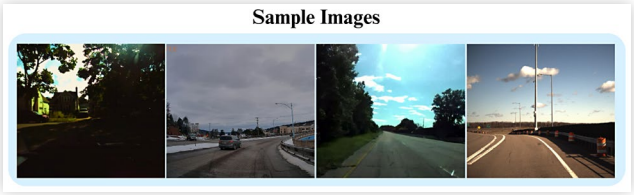

of lanes, weather conditions, and road diversity. This diversity makes the YOLOv8 model capable of detecting lane markings with good accuracy for a wide range of world conditions enabling it to be highly effective for autonomous vehicle applications.

Custom YOLOv8 Model Training

The lane detection model employed in this study was trained on YOLOv8. While the YOLOv8 model used is not novel in this study, its application to lane segmentation in autonomous driving offers clear advantages. YOLOv8 excels in object detection and image segmentation tasks, especially where real-time processing is essential. Its low latency ensures smooth, real-time lane segmentation, even in dynamic environments with variations in lighting, weather, and road conditions.

The segmentation provided by YOLOv8 is crucial for calculating the lateral offset of vehicles. After detecting lane markings, the model generates a segmented area representing the driving lane. The system computes the left and right lane boundaries from this segmented area, enabling centimeter-level offset calculations that are fed into the lateral offset estimation system.

The YOLOv8 model showed stable training and validation losses across different metrics such as box loss, segmentation loss, class loss, and DFL loss, as illustrated in figure 3. The training and validation loss curves demonstrate the model's learning progression and convergence over the epochs. The key performance metrics are summarized in table 1.

FIGURE 3 Training and Validation Loss Curves for YOLOv8

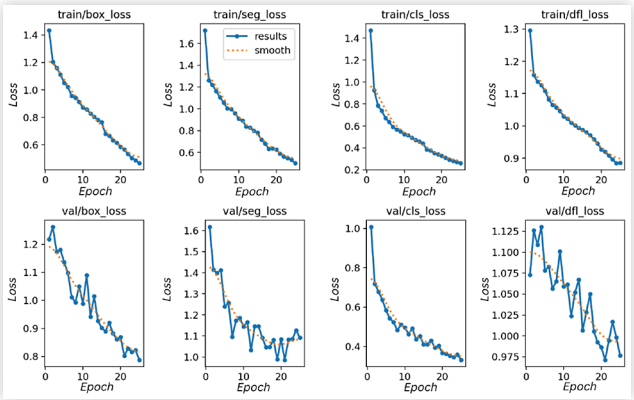

TABLE 1 YOLOv8 Lane Segmentation Performance Metrics

Metric	Value
Precision	0.99
Recall	0.98
mAP50	0.995
mIoU	0.95

This strong performance in precision and recall reflects the model's ability to accurately detect lanes with minimal errors, supporting its use in autonomous driving systems.

Novel Calibration and Offset Estimation

A main contribution of this work is the calibration method that converts the YOLOv8 lane detection results from image coordinates into world coordinates system. This method ensures accurate lateral offset estimation, essential for maintaining vehicle position within the lane.

As shown in figure 4, in our proposed calibration process, aligned with vehicle perspective as captured by the onboard camera, we considered nine reference markers positioned in front of the vehicle. These markers are organized into three sets: L_1, L_2, L_3 for the left edge of the vehicle, C_1, C_2, C_3 for the centerline of the vehicle, and R_1, R_2, and R_3 for the right edge of the vehicle. To identify the vehicle left and right edges, we rely on the passenger and driver sides wheels, while the steering wheel is set to zero using commands available through the Drive-by-Wire system. Based on the left and right boundaries, we determine the vehicle centerline based on three middle points with preselected distances from front bumper.

FIGURE 4 Perspective and Camera View of the Calibration Markers for Lane Offset Estimation

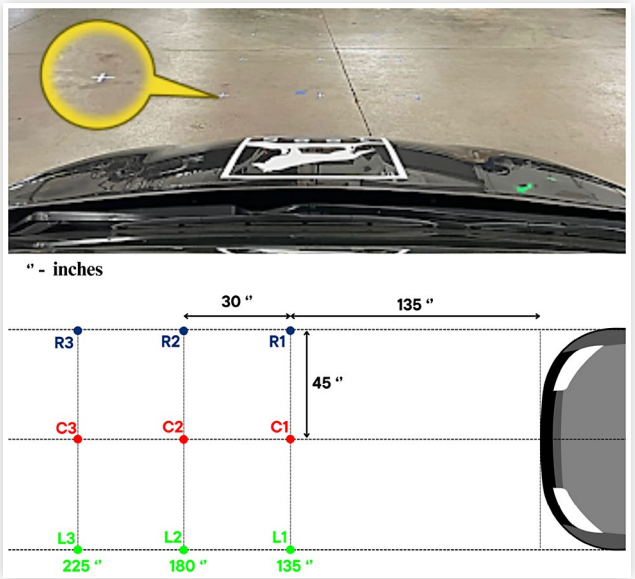

Figure 4 upper section shows the schematic of top view of these markers, and the lower section illustrates how the markers appear in image frame. Including three markers in each set allows us to minimize the error in estimating the vehicle centerline, and right and left edges in an image frame.

Lateral Offset Calculation - To compute the lateral offset of the vehicle from the lane center, a series of steps are followed using regression lines and intersection points. Figure 5 illustrates the relationship between the calibration points and regression lines for calculating the offset from the lane center.

The line l_{h1} represents a reference line in the segmented lane area, which is crucial for calculating the lateral offset of the vehicle. From Figure 5, the green segmented area is the output of the trained YOLOv8 model. The points $P_{l(h1)}$ and $P_{r(h1)}$ are the left and right endpoints of this line l_{h1} which is considered in the segmented area to estimate the lateral offset, while $P_{c(h1)}$ is the center point of the line. This center point corresponds to the actual center of the lane.

Step 1: *Regression lines for left, center, and right calibration points* For the calibration, regression lines are fitted to the left, center, and right reference points. These lines represent the vehicle boundaries and the centerline, and are described as,

$$\begin{aligned} l_i &= a_i u + b_i v + c_i \\ i &\in \{L,C,R\} \end{aligned} \tag{1}$$

Where: a_i, b_i, c_i are the coefficients of the regression line

Step 2: *Reference Line l_{h1} Intersection points*

The reference line l_{h1} is defined by the endpoints $(u_{l(h1)}, v_{l(h1)})$ and $(u_{r(h1)}, v_{r(h1)})$. It is expressed in slope-intercept form:

$$\begin{aligned} l_{h1} &: v = m_{h1} u + b_{h1} \\ \text{Where} &: m_{h1} = \frac{v_{r(h1)} - v_{l(h1)}}{u_{r(h1)} - u_{l(h1)}}, \quad b_{h1} = v_{l(h1)} - m_{h1} u_{l(h1)} \end{aligned} \tag{2}$$

The intersection points (P_L, P_C, P_R) between the regression lines and l_{h1} are calculated by solving:

FIGURE 5 Regression Lines and Intersection Points for Lateral Offset Calculation

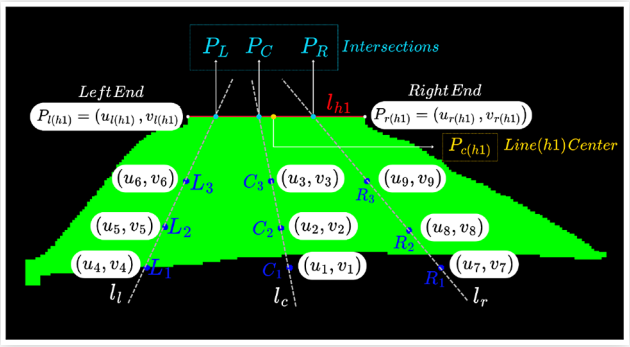

$$\begin{aligned} a_i u + b_i \left(m_{h1} u + b_{h1}\right) + c_i &= 0 \\ i &\in \{L,C,R\} \end{aligned} \tag{3}$$

Simplifying for u:

$$u_{P_i} = \frac{-b_i b_{h1} - c_i}{a_i + b_i m_{h1}} \tag{4}$$

The corresponding v-coordinate is given by:

$$v_{P_i} = m_{h1} u_{P_i} + b_{h1} \tag{5}$$

These intersection points are critical for calculating the vehicle lateral position.

Step 3: *Distances between intersection points and reference points* To quantify the lateral offset, we calculate distances between the intersection points and the reference center point $P_{c(h1)}$. Additionally, we need to calculate the distances between the intersection points themselves on the line l_{h1}. Distance between P_C and $P_{c(h1)}$ is given by:

$$\begin{aligned} d_i &= \sqrt{\left(u_{P_c} - u_{P_{c(h1)}}\right)^2 + \left(v_{P_c} - v_{P_{c(h1)}}\right)^2} \\ i &\in \{L,C,R\} \end{aligned} \tag{6}$$

$$\begin{cases} d_{h1_L} = \| P_L - P_C \| \\ d_{h1_R} = \| P_R - P_C \| \end{cases} \tag{7}$$

Step 4: *Offset calculation in pixels*

Based on the calculated distances, the final lateral offset values for the center left, and right points are computed as,

$$\begin{cases} d_{o_C} = d_C & \text{center} \\ d_{o_R} = d_R - d_{h1_R} & \text{right} \\ d_{o_L} = d_L - d_{h1_L} & \text{left} \end{cases} \tag{8}$$

Step 5: *Final offset calculation in pixels*

The lateral offset in pixel values is determined by averaging the offset values for the center, left, and right points:

$$\hat{d}^p_{o_{h_1}} = \frac{d_{o_C} + d_{o_L} + d_{o_R}}{3} \tag{9}$$

Step 6: *Converting offset from pixels to meters*

Finally, to convert the pixel-based offset to word coordinates in meters, we use the following conversion formula based on the standard lane width of 3.6 meters:

$$\hat{d}^m_{o_{h_1}} = \hat{d}^p_{o_{h_1}} \times \frac{3.6[\text{m}]}{d_{L_R}} \tag{10}$$

Where d_{LR} is the distance between the $P_{l(h1)}$ and $P_{r(h1)}$, that are the endpoints of the line l_{h1}. This method ensures precise calculation of the lateral offset in world coordinates, enhancing vehicle control and safety during lane following.

Using Multiple Reference Lines for Improved Offset Calculation

To improve the accuracy of the lateral offset estimation, multiple reference lines are considered at different vertical levels in the segmented lane area. By incorporating multiple lines, the system can minimize errors caused by detection noise or small variations in lane boundaries. Each of these reference lines is processed in the same manner as l_{h1} calculating the intersection points with the regression lines l_C, l_L, and l_R.

For each reference line l_{h_i} (where i = 1,2,3,...,n) the final offset value in meters, $\hat{d}^m_{o_{h_i}}$, is calculated. The final lateral offset is obtained by averaging the values across all the reference lines to reduce the impact of noise and improve accuracy. The final offset is given by:

$$\hat{d}^m_o = \frac{1}{n}\Sigma^n_{i=1}\hat{d}^m_{o_{h_i}} \quad (11)$$

Where n is the number of reference lines considered in the segmented area.

This approach ensures that the offset value is robust and consistent, mitigating any inaccuracies caused by environmental factors or slight deviations in the lane detection process.

Model Assessment and Implementation

The model was implemented on an instrumented L4/5 capable autonomous vehicle, and a comprehensive set of tests was conducted to evaluate lane detection and lateral offset estimation performance. The tests took place at the American Center for Mobility, which is designed to simulate world driving conditions, including variations in road surface quality, lighting, and environmental factors such as Normal, Underexposed, and Snow. The results of these tests provide critical insights into the model's robustness, accuracy, and real-time applicability in autonomous vehicle deployment.

Lane Detection Model Performance Analysis

The initial testing phase involved evaluating the YOLOv8 segmentation model on 200 images. Although the YOLOv8 model is not a novel aspect of this project, it plays a crucial role in the overall offset calculation by providing reliable lane segmentation. The model's output directly impacts the accuracy of the offset measurement, making its performance vital to the system.

Figure 6 shows examples of the model's output across different driving conditions. As seen in the images,

FIGURE 6 Lane Detection model output across different driving conditions

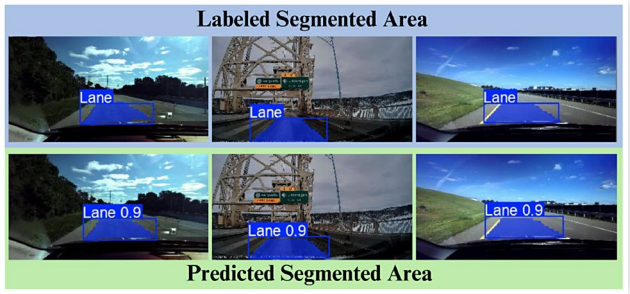

the blue-shaded areas represent the detected lanes, with confidence scores of 0.9. These results demonstrate the model's ability to consistently detect lanes under varied environmental conditions, such as clear skies, complex bridge structures, and different road surfaces. The high confidence score for lane detection ensures reliable input for subsequent offset calculations.

Figure 6 and the performance metrics in table 2 show that the model detected 199 lanes correctly with only one misclassification, yielding a high precision and recall of 99.5%. This strong performance ensures that the model provides accurate lane segmentation, which is essential for calculating the vehicle's lateral offset.

The results from the initial testing phase confirm that the YOLOv8 segmentation model performs effectively across diverse conditions. The high confidence in lane detection, along with the robust precision and recall metrics, indicate that the model is well-suited for providing input to the offset calculation process.

GPS-Based Offset to Centerline Estimation Model Analysis

To assess the performance of the proposed model, we collected GPS with RTK correction and camera data while driving a road with a High-definition map (HD Map). In this test procedure, GPS location of the lane markings, and vehicle accurate position information provides sufficient information to measure the offset of the test vehicle to the centerline of the lane. Here we present the model assessment result and discussion for three trials. In each trial, we drove the test vehicle on a straight road while swinging left and right. To mitigate the biased error, we drove the test vehicle on a straight line and compared the mean of two offsets, derived from GPS data, and estimated by the proposed model. This step allow us to minimize the impact of GPS drift error on our model assessment. It is important to note that the true offset to the centerline derived from GPS is also subjected to errors due to inaccuracies in RTK corrections.

Figure 7-(a) shows the relationship between the true offset and the error. The red trendline shows a linear relationship with a slope of 0.4, indicating a positive correlation between the true offset and error, which means model underestimates the offset. Considering the 99.5%

FIGURE 7 Offset to centerline estimation model assessment results.

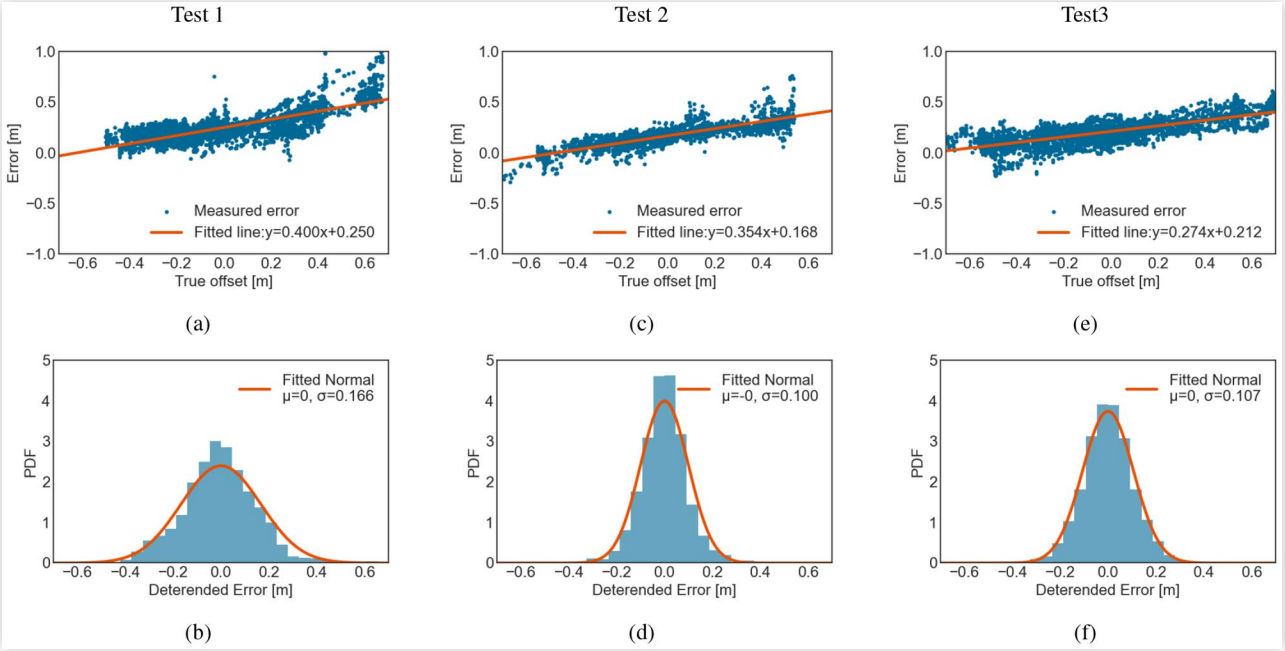

Yolo model accuracy in detecting the lane boundary (see table 2), the source of this error can be found in (10). In this equation, the distance between left and right hand side lane markings in camera horizon is considered a constant; while, lane width varies with road type, and more importantly, distance between lane markings in camera horizon correlates with vehicle relative yaw angle to centerline. We calculate the detrended error as:

$$e_{\text{deterended}} = d_{\text{true}} - \frac{\hat{d} + i}{(1 - s)} \tag{12}$$

where d_{true} is derived from GPS data, $\hat{d}$ is the model estimation after mitigating biased error, and s and i refer to the slope and intercept of the fitted line.

Figure 7-(b) shows that the zero mean deterended error distribution for T1 with a standard deviation (STD) of 16.6. The deterended error, known as random walk error, can be calculated using calculated trends in error in 7-(a). Figure 7-(c) shows that the error in second trail also has a linear trend, with a slope of 0.35. Compared to T1, the scatter plot and the histogram demonstrates a narrower distribution of deterended errors; however, the linear trend persists, suggesting a similar underestimation of offset in the second trial. In figure 7-(d) the T2 histogram shows a standard deviation of 10.0. In 7-(e), the slope of the linear relationship is 0.27, which is similar correlation between the true offset and the error, to the previous trials. The error distribution in figure 7-(f) for T3 has a standard deviation of 10.7 compared, suggesting that random walk error power is slightly higher in the third trial.

Figure 8 presents the error characteristics for the union of three tests data. According to this figure, the overall biased error in these tests is 21.4 cm and the slope is 0.328. As discussed earlier, both GPS data and proposed model contribute to the biased error. Also the bias error can simply be measured and mitigated by driving the vehicle on a single lane and measuring the average offset to the centerline.

Finally, we can model the error in estimated offset to centerline as:

$$\begin{gathered} \hat{d} = d_{\text{true}} - e_{\text{scale}} \times d_{\text{true}} + e_{\text{random walk}} + e_{\text{bias}} \\ e_{scale} = 0.328 \\ e_{\text{randoen walk}} \sim N(0, 0.135) \\ e_{\text{bias}} = 21.4cm \end{gathered} \tag{13}$$

where e_{scale} is the slope of the fitted line to union of measured errors in all three trials, $e_{\text{random walk}}$ is calculated STD of union deterended error, and e_{bias} is the biased error. Using this step by step analysis, we can measure the biased and scaling errors and mitigate these factors in the final estimation. Accordingly, in future work, we will integrate the described procedure into the calibration process and enhance the proposed model performance in estimating the vehicle offset to lane centerline using a

TABLE 2 YOLOv8 Lane Segmentation Testing Performance Metrics

Metric	Value
True Positives	199
False Negatives	1
True Negatives	0
False Positives	0
Precision	99.5%
Recall	99.5%
Accuracy	99.5%

FIGURE 8 Error analysis for trials union set, i.e., {*T*1 ∪ *T*2 ∪ *T*3}.

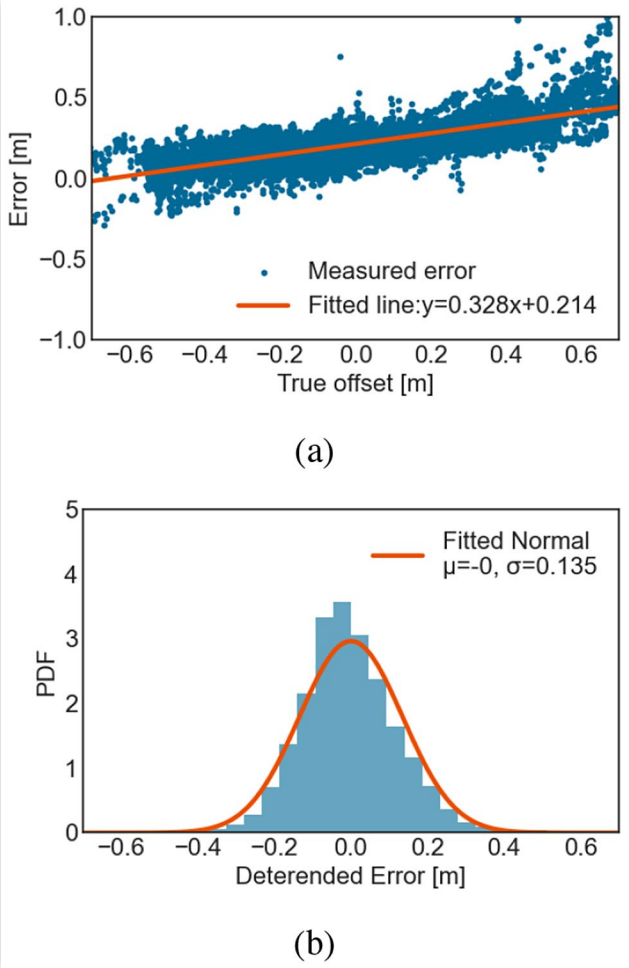

TABLE 3 Summary of Test Results for YOLOv8 Lane Detection Model Performance

Test	Mean Processing Time (ms)	Sample Size	e_{scale}	e_{bias}	STD($e_{random\ walk}$)
T1	14.4	4103	0.400	0.250	0.166
T2	13.6	3053	0.354	0.168	0.100
T3	14.0	4685	0.274	0.212	0.107
{*T*1 ∪ *T*2 ∪ *T*3}	14.04	11841	0.328	0.214	0.135

monocular camera. A summary of perfomance analysis discussion is presented in Table 3.

Conclusion

In this research, we proposed a lane detection and offset estimation system tailored for real-time applications in autonomous driving. The system utilizes a custom YOLOv8 model for lane segmentation, followed by a novel offset estimation approach that achieves centimeter-level accuracy in calculating the lateral position of the vehicle relative to the lane. The combination of accurate lane detection and precise offset estimation makes this system robust across diverse driving conditions, including scenarios with no visible lane markings. The system operates at a consistent speed of 30 FPS, ensuring smooth, real-time performance in dynamic driving environments.

Experimental results demonstrate that the system not only accurately detects lanes but also reliably computes the vehicle's offset from the lane center with high precision. The centimeter-level offset accuracy, achieved through a nine-point calibration method, ensures that the vehicle maintains safe positioning within the lane. Future work will focus on further refining the model's capability to handle more complex road conditions and improving the real-world applicability of the system for fully autonomous driving scenarios.

References

1. Schexnaydre, L. et al., "Using Automated Vehicle Positioning to Improve Efficiency in Vehicle Platooning," in *Autonomous Systems: Sensors, Processing, and Security for Ground, Air, Sea, and Space Vehicles and Infrastructure 2023*, 12540. SPIE, 2023.
2. Pavel, M.I., Tan, S.Y., and Abdullah, A., "Vision-Based Autonomous Vehicle Systems Based on Deep Learning: A Systematic Literature Review," *Applied Sciences* 12, no. 14 (2022): 6831.
3. Wang, J.-G., Lin, C.-J., and Chen, S.-M., "Applying Fuzzy Method to Vision-Based Lane Detection and Departure Warning System," *Expert Systems with Applications* 37, no. 1 (2010): 113-126.
4. Hsiao, P.-Y. et al., "A Portable Vision-Based Real-Time Lane Departure Warning System: Day and Night," *IEEE Transactions on Vehicular Technology* 58, no. 4 (2008): 2089-2094.
5. Wang, X., Wang, Y., and Wen, C., "Robust Lane Detection Based on Gradient-Pairs Constraint," in *Proceedings of the 30th Chinese Control Conference*, IEEE, 2011.
6. Duan, J., Zhang, Y., and Zheng, B., "Lane Line Recognition Algorithm Based on Threshold Segmentation and Continuity of Lane Line," in *2016 2nd IEEE International Conference on Computer and Communications (ICCC)*, IEEE, 2016.
7. Gaikwad, V. and Lokhande, S., "Lane Departure Identification for Advanced Driver Assistance," *IEEE Transactions on Intelligent Transportation Systems* 16, no. 2 (2014): 910-918.
8. Mu, C. and Ma, X., "Lane Detection Based on Object Segmentation and Piecewise Fitting," *TELKOMNIKA Indonesian Journal of Electrical Engineering* 12, no. 5 (2014): 3491-3500.
9. Ding, D., Leem, C., and Lee, K-y., "An Adaptive Road ROI Determination Algorithm for Lane Detection," in *2013*

IEEE International Conference of IEEE Region 10 (TENCON 2013), IEEE, 2013.

10. Wu, P.-C., Chang, C.-Y., and Lin, C.H., "Lane-Mark Extraction for Automobiles under Complex Conditions," *Pattern Recognition* 47, no. 8 (2014): 2756-2767.
11. Aung, T., and Zaw, M.H., "Video Based Lane Departure Warning System Using Hough Transform," in *International Conference on Advances in Engineering and Technology*, Citeseer, 2014.
12. Niu, J. et al., "Robust Lane Detection Using Two-Stage Feature Extraction with Curve Fitting," *Pattern Recognition* 59 (2016): 225-233.
13. McCall, J.C. and Trivedi, M.M., "Video-Based Lane Estimation and Tracking for Driver Assistance: Survey, System, and Evaluation," *IEEE Transactions on Intelligent Transportation Systems* 7, no. 1 (2006): 20-37.
14. Wang, Y., Shen, D., and Teoh, E.K., "Lane Detection Using Spline Model," *Pattern Recognition Letters* 21, no. 8 (2000): 677-689.
15. Fu, M. et al., "Multi-Lanes Detection Based on Panoramic Camera," in *11th IEEE International Conference on Control & Automation (ICCA)*, IEEE, 2014.
16. Li, Y. et al., "Nighttime Lane Markings Recognition Based on Canny Detection and Hough Transform," in *2016 IEEE International Conference on Real-time Computing and Robotics (RCAR)*, IEEE, 2016.
17. Zhang, R. et al., "RS-Lane: A Robust Lane Detection Method Based on ResNeSt and Self-Attention Distillation for Challenging Traffic Situations," *Journal of Advanced Transportation* 2021, no. 1 (2021): 7544355.
18. Munir, F. et al., "LDNet: End-to-End Lane Marking Detection Approach Using a Dynamic Vision Sensor," *IEEE Transactions on Intelligent Transportation Systems* 23, no. 7 (2021): 9318-9334.

Acknowledgments

This work is sponsored by Advanced Research Projects - Energy (ARPA-E) of the U.S. Department of Energy (DOE) under award number DE-AR0000788. Stellantis is the industry partner and has played an important role with technical support and guidance.

ISSN 0148-7191